Chemistry Europe
European Chemical Societies Publishing

WILEY VCH

Excellence in Chemistry Research

Announcing our new flagship journal

- Gold Open Access
- Publishing charges waived
- Preprints welcome
- Edited by active scientists

Meet the Editors of *ChemistryEurope*

Luisa De Cola
Università degli Studi di Milano Statale, Italy

Ive Hermans
University of Wisconsin-Madison, USA

Ken Tanaka
Tokyo Institute of Technology, Japan

ChemCatChem

Research Article
doi.org/10.1002/cctc.202300821

Chemistry Europe
European Chemical Societies Publishing

www.chemcatchem.org

Light-Driven NADPH Cofactor Recycling by Photosystem I for Biocatalytic Reactions

Hitesh Medipally,[a] Alice Guarneri,[b] Lars Pospisil,[a] Maurice C. R. Franssen,[b] Willem J. H. van Berkel,[c] Caroline E. Paul,*[d] and Marc M. Nowaczyk*[a, e]

Biocatalytic asymmetric reduction of C=C and C=O bonds is highly attractive to produce valuable (chiral) chemicals for the fine and pharmaceutical industry, yet occurs at the expense of reduced nicotinamide adenine dinucleotide coenzyme NADPH that requires recycling. Established methods each have their challenges. Here we developed a light-driven approach based on photosystem I (PSI) by mimicking the natural electron transfer from PSI via ferredoxin (Fd) towards ferredoxin $NADP^+$ reductase (FNR) in vitro. Illumination with red light led to reduction of $NADP^+$ to NADPH with a turnover frequency of 2.55 s^{-1} (> 9000 h^{-1}) at pH 7.5. Light-driven NADPH regeneration by PSI-Fd-FNR was coupled with three oxidoreductases for asymmetric reduction of C=C and C=O bonds, reaching up to 99% conversion with a turnover number of 3035, and retaining enantioselectivity. This study demonstrates the capacity of a PSI system to drive continuous NADPH-dependent biocatalytic conversions with light.

Introduction

Biocatalysts display exquisite efficiency, chemo-, enantio- and regioselectivity to synthesize a wide variety of chemicals under mild and economically sustainable conditions.[1] Oxidoreductases are one of the industrially most important classes of enzymes after hydrolases, and amount to approximately one-third of the reported enzymes in the BRaunschweig ENzyme DAtabase (BRENDA).[2] Many relevant in vitro oxidoreductase-catalyzed reactions require the continuous supply of nicotinamide adenine dinucleotide NAD(P)H as reductant and its recycling due to cost and stability.[3] Over the last decades enzymatic, electrochemical, and photochemical recycling systems have been developed,[4] with the enzymatic approach being favored. The most commonly used NAD(P)H recycling enzymes in laboratory or industrial scale include NAD- or NADP-dependent oxidoreductases such as glucose dehydrogenase (GDH), glucose-6-phosphate dehydrogenase (G6PDH), formate dehydrogenase (FDH), phosphite dehydrogenase (PTDH), alcohol dehydrogenase (ADH), and hydrogenase (Hyd). Some of these recycling systems have poor atom efficiency: GDH, G6PDH, or display low activity: FDH, PTDH, and Hyd.[5] Moreover, few enzymes are naturally NADP-dependent such as GDH, G6PDH and specific ADHs, limiting the pool of options for NADPH regeneration.

In contrast, the photosynthetic electron transport chain in cyanobacteria, algae and plants acts as an excellent platform for sustainable and efficient NADPH recycling, with water used as the primary electron donor.[6] Despite this advantage, its dependency on light for growth, a limited substrate scope due to the selective membrane barrier and low production rates make the in vivo photosynthetic system inefficient compared with other optimized heterotrophic production systems.[6b,7] In photosynthetic electron transfer, photosystem I (PSI) acts as a light-driven electron pump, which is reduced by plastocyanin (PC) or cytochrome c_6 ($Cytc_6$), and which provides electrons for NADPH recycling via ferredoxin (Fd) and ferredoxin $NADP^+$ reductase (FNR). The ultimate electron source for this process in the natural system is the water-splitting activity of photosystem II (PSII). Here, we developed the proof-of-concept for a light-driven in vitro system for NADPH recycling by coupling of isolated PSI,[8] Fd,[9] FNR,[10] with three different oxidoreductases (Figure 1).

Our recycling system was assembled by artificial reconstitution of the photosynthetic electron transport chain in vitro, thus mimicking the cathodic half-cell reaction of natural photosynthesis.[11] In the PSI-driven biocascade, the difference in reduction potentials (E_M) of the used compounds provides a paradigm for sequential electron transfer (Figure 2a). NaAsc (E_M: +0.078 V vs. a standard hydrogen electrode SHE) is used as a

[a] H. Medipally, L. Pospisil, Prof. Dr. M. M. Nowaczyk
Molecular Mechanisms of Photosynthesis, Faculty of Biology and Biotechnology, Ruhr-University Bochum, Universitätsstr. 150, 44801 Bochum (Germany)
[b] Dr. A. Guarneri, Prof. Dr. M. C. R. Franssen
Laboratory of Organic Chemistry, Wageningen University, Stippeneng 4, 6708 WE Wageningen (The Netherlands)
[c] Prof. Dr. W. J. H. van Berkel
Laboratory of Food Chemistry, Wageningen University, Bornse Weilanden 9, 6708 WG Wageningen (The Netherlands)
[d] Prof. Dr. C. E. Paul
Department of Biotechnology, Delft University of Technology, van der Maasweg 9, 2629 HZ, Delft (The Netherlands)
E-mail: c.e.paul@tudelft.nl
Homepage: http://www.tudelft.nl/bt/cepaul
[e] Prof. Dr. M. M. Nowaczyk
Department of Biochemistry, University of Rostock, Albert-Einstein-Str. 3, 18059 Rostock (Germany)
E-mail: marc.nowaczyk@uni-rostock.de
Homepage: http://www.biochemie.uni-rostock.de/

Supporting information for this article is available on the WWW under https://doi.org/10.1002/cctc.202300821

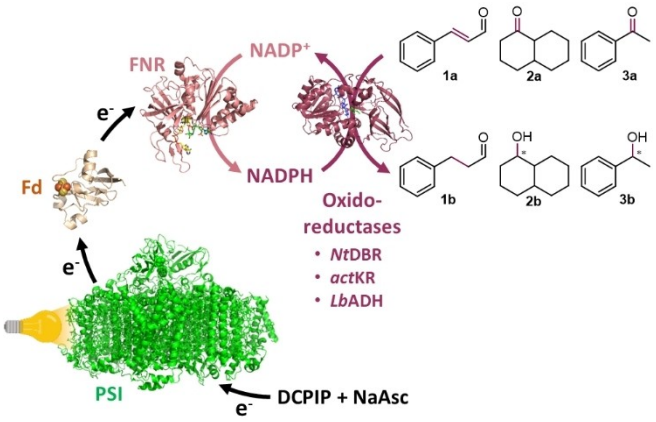

Figure 1. Light-driven NADPH cofactor recycling by PSI-Fd-FNR for redox biocatalysis. NaAsc: sodium ascorbate, DCPIP: dichlorophenolindophenol, PSI: photosystem I (PDB: 1JBO), Fd: ferredoxin (PDB: 5AUI), FNR: ferredoxin $NADP^+$ reductase (PDB: 1GJR), $NADP^+$: nicotinamide adenine dinucleotide phosphate, *Nt*DBR: *Nicotiana tabacum* double bond reductase, *act*KR: actinorhodin ketoreductase from *Streptomyces coelicor*, *Lb*ADH: *Lactobacillus brevis* alcohol dehydrogenase.

sacrificial electron donor, and DCPIP (E_M: +0.228 V vs. SHE) acts as an electron mediator to PSI. Light-driven charge separation within PSI generates a strong reducing potential (E_M: −1.3 V vs. SHE), thus enabling electron transfer to Fd (E_M: −0.43 V vs. SHE) via the terminal 4Fe-4S cluster (F_B) of PSI. The single electron carrier Fd donates two electrons, one at each time to the FAD cofactor (E_M: −0.38 V vs. SHE) of FNR, for the full reduction of $NADP^+$ to NADPH.

Similar PSI-driven biocascade reactions have been reported previously as classical photoreduction assays for FDH,[11] FNR,[12] and Hyd.[13] Here we extended the scope of a PSI-biocascade and explored its ability as an NADPH recycling system. Three different oxidoreductases were coupled to demonstrate NADPH regeneration with PSI-Fd-FNR for asymmetric C=C and C=O reduction: i) *Nicotiana tabacum* double bond reductase (*Nt*DBR, EC 1.3.1.102), which reduces *trans*-cinnamaldehyde **1a** to dihydrocinnamaldehyde **1b**;[14] ii) actinorhodin ketoreductase from *Streptomyces coelicolor* (*act*KR, EC 1.1.1.184) that converts 1-decalone **2a** to 1-decalol **2b**;[15] and iii) alcohol dehydrogenase from *Lactobacillus brevis* (*Lb*ADH, EC 1.1.1.1)[16] to reduce acetophenone **3a** to (*R*)-phenylethanol **3b** (Figure 1).

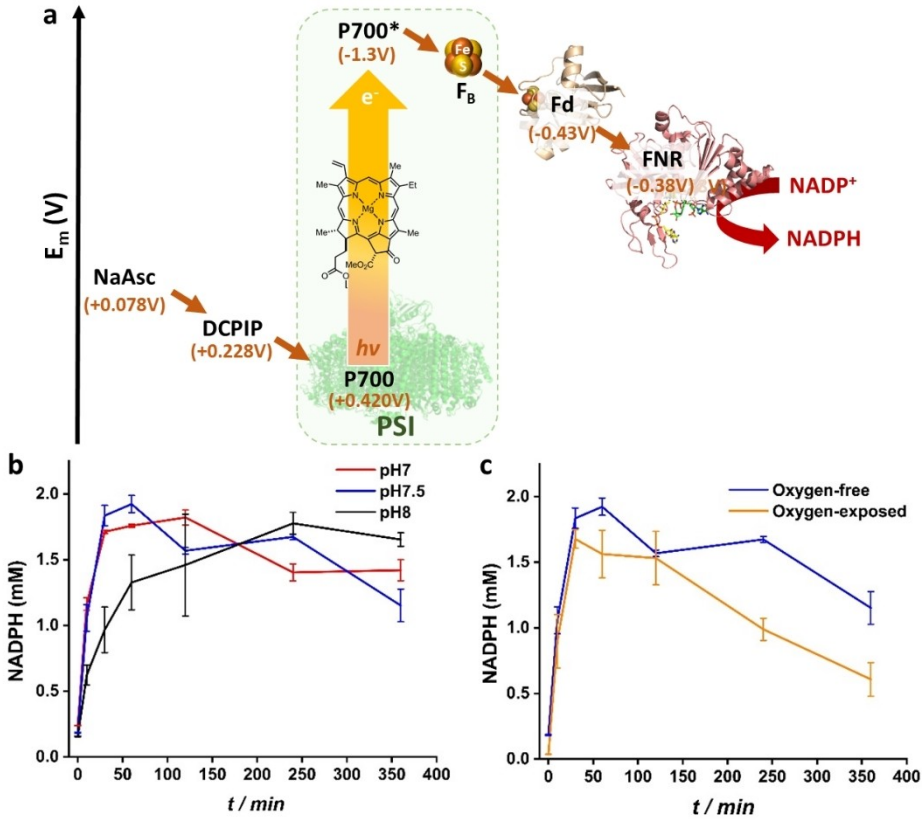

Figure 2. a) Schematic representation of electron transfer in the PSI-Fd-FNR cascade. Midpoint potential values are according to literature references vs. SHE;[12,17] b) pH-dependent production of NADPH by the PSI-Fd-FNR cascade. Conditions: 0.57 μM PSI (50 μg chlorophyll (Chl), 1 μM FNR, 4 μM Fd, 3 mM $NADP^+$, 100 mM NaAsc, 0.8 mM DCPIP, buffer (black: 50 mM: MOPS-NaOH pH 7.0; red: 50 mM Tris-HCl pH 7.5; blue: 50 mM Tricine buffer pH 8.0 + 3.0 mM NaCl + 0.03 % *n*-dodecyl-β-maltoside, red light (λ = 685 nm, 500 μmol $m^{-2} s^{-1}$), 100 rpm, reaction volume 1 mL. c) Influence of molecular oxygen on NADPH production by the PSI-Fd-FNR cascade. NADPH production was monitored in aerobic (yellow line) and oxygen-free (blue line) conditions over time (0 to 6 h). Conditions: 0.57 μM PSI (50 μg Chl), 1 μM FNR, 4 μM Fd, 3 mM $NADP^+$, 100 mM NaAsc, 0.8 mM DCPIP, Tris-HCl buffer pH 7.5, red light (λ = 685 nm, 500 μmol $m^{-2} s^{-1}$), 100 rpm, 1 mL reaction volume, 25 °C. All experiments were performed in triplicate, error bars represent standard deviation.

In nature, PSI is embedded in the thylakoids, exposing one side of the complex to the basic stromal pH and the other end to the acidic luminal pH. The pH of the chloroplast lumen varies in the range of 5.8 to 6.5 under moderate light conditions. On the other hand, the stromal side pH is in the range of 7.8 to 8.0,[18] which makes it difficult to predict the optimal pH conditions for NADPH production in vitro. Therefore, we monitored the light-driven NADPH generation capacity of PSI-Fd-FNR at different pH conditions by measuring the concentration of NADPH at various time intervals over 6 h (Figures 2b, S3, S8 and S9).

The reduction rate of $NADP^+$ to NADPH at pH 7.0, 7.5 and 8.0 were determined to be 1.51, 1.73, and 1.17 mM/h, respectively, with the best turnover frequency (TOF) of 2.55 s^{-1} (9180 h^{-1}) at pH 7.5. A rapid increase in NADPH concentration was observed in the initial 30 min of the reaction, especially at pH 7.0 and 7.5, and slightly slower at pH 8.0. The small differences in the initial rates can be attributed to the different pH dependencies of the individual electron transfer steps in the cascade. The interaction of Fd with PSI is mainly entropy driven and therefore less affected by pH,[19] whereas the interaction of PSI with its natural electron donors, PC, and Cytc_6, is driven by hydrophobic and electrostatic interactions with an optimum at acidic pH.[20] However, the artificial electron donors NaAsc and DCPIP behave differently in the in vitro cascade. DCPIP is in a reduced state ($DCPIPH_2$) due to the presence of excess NaAsc (100 mM). The lack of net charge and the aromatic nature of $DCPIPH_2$ make it also a potential candidate for hydrophobic interaction with the donor site of PSI. NaAsc itself is known to donate electrons to the PSI donor site very slowly in its deprotonated state.[17a] Thus, all electron transfer reactions in the system are mainly based on hydrophobic interactions, which explains the minor influence of the pH, with an optimum at pH 7.5 (see also Figures S1 and S2 for detailed information on electron transfer steps and protein-protein interactions within the biocascade).

Once the optimal pH was determined, we tested the influence of molecular oxygen on the PSI-Fd-FNR biocascade. Both the electron donor NaAsc and $NADP^+$ are relatively stable in the presence of O_2 but other components such as PSI,[17a] Fd,[21] and FNR,[22] are known to produce reactive oxygen species. To avoid these side reactions, all PSI-Fd-FNR bioconversions were performed in an O_2-free environment (<10 ppm) (Figure 2c). However, to investigate the effect of O_2 on NADPH production, PSI-Fd-FNR was also exposed to air (pH 7.5, ordinary laboratory conditions) and the results were compared to a measurement in an O_2-free environment (Figure 2c). Interestingly, there was no significant difference in the initial rate of NADPH production in both reaction conditions. This indicates that the electron transfer between PSI, Fd, and FNR is highly streamlined due to the high concentration of O_2 in the natural system, which is in agreement with previous results.[23]

The streamlined electron transfer can be explained by fast electron transfer within PSI,[24] a higher second-order rate constant of the interaction between PSI and Fd compared to O_2, which are 3.5×10^8 $M^{-1}s^{-1}$ and 7.5×10^4 $M^{-1}s^{-1}$, respectively,[25] and a higher second-order rate constant of the interaction of Fd with FNR (6.2×10^8 $M^{-1}s^{-1}$),[12] which is faster than the re-oxidation of Fd by dissolved O_2.[21] As a result, this streamlined electron transfer prevents interference by O_2 in the presented PSI-Fd-FNR cascade. On the other hand, upon longer incubation under aerobic conditions, a faster decrease in NADPH concentration was observed than in the absence of O_2 (Figure 2c).

FNR is known to have a reversible function and can also oxidize NADPH in the presence of an electron acceptor.[22] In the PSI-Fd-FNR system, Fd_{ox},[26] $DCPIP_{ox}$,[27] and O_2 could play such a role, however $DCPIP_{ox}$ is short-lived due to the immediate reduction by NaAsc[28] and Fd_{ox} is expected to be rapidly reduced by PSI. Thus, the stronger decline in NADPH concentration under aerobic conditions might be related to the NADPH oxidase activity of FNR, which includes the reaction of O_2 with the reduced flavin adenine dinucleotide (FAD) cofactor of FNR. Additionally, the decreases in NADPH concentration could be due to the decomposition of NADPH over time. The faster decline in NADPH concentration was observed at pH 7.0 and pH 7.5 compared with pH 8.0 (Figure 1b), indicating that the NADPH decomposition is pH dependent.[29] The comparison of PSI-Fd-FNR-mediated NADPH generation with other commonly used enzymes demonstrates the applicability of our approach (Table 1).

PSI-Fd-FNR outperformed the turnover number of FDH and PTDH by two to four-fold. Additionally, PSI-Fd-FNR clearly excelled over other light-driven NADPH recycling systems, which are based on FNR quantum dot fusions (FNR-QD),[33] and a graphene-based photocatalyst with a $[Cp^*Rh(bpy)Cl]^+$ complex (Graphene photocat-Rh)[34] (Table 1). Also the turnover number (TON) of PSI-Fd-FNR, calculated based on 1 h time points, was determined to be 3035, indicating the robustness of the system. With a series of optimizations, the NADPH generation capacity of PSI-Fd-FNR could be further improved, e.g. by optimizing the stoichiometry of PSI, Fd and FNR, as well as by improving the rate of the individual electron transfer steps. The rate constant for $DCPIPH_2$ mediated reduction of the oxidized P_{700} reaction center of PSI under continuous illumination was reported to be 1.9×10^8 $M^{-1}s^{-1}$ at pH 8.0 with methyl viologen as the final electron acceptor,[35] which is less than the rate constant of Fd reduction by PSI (as mentioned above) and clearly the rate-limiting step in electron transfer of the system. Additionally, the electron transfer rates of $DCPIPH_2$ and NaAsc are diffusion limited. Thus, isotropic immobilization of PSI on an electrode surface and efficient electronic coupling by redox-active hydrogels, as shown previously,[36] may also improve electron donation to the PSI-Fd-FNR cascade.

To further compare the different NADPH recycling systems, the performance of each system was evaluated based on additional parameters such as atom efficiency and simplicity of product isolation (Table 1). As a result, FDH and PTDH appear more promising compared to GDH, FNR-QD and PSI-Fd-FNR. In the case of FDH, CO_2 is formed as a by-product and easily removed, whereas PTDH forms phosphate, which can also be easily separated via calcium precipitation. The by-products obtained in the case of graphene photocatalyst, GDH, FNR-QD and PSI-Fd-FNR are diethanolamine, gluconolactone/gluconic

Table 1. Comparison of PSI-Fd-FNR with other NADPH recycling catalysts, and relative comparison of performance.

NADPH generation catalyst	k_{cat} (s^{-1})	K_M (mM)	k_{cat}/K_M ($s^{-}mM^{-}$)	TON[b]	pH	Organism	Electron transfer steps	Electron donor	k_{cat}/K_M or TON (NADPH)[e]	Atom efficiency	Ease of work-up	Ref.
PSI-Fd-FNR	2.55[a]	n.a.	n.a.	3035	7.5	*T. vestitus* BP1	4	sodium ascorbate	++	–	+	this study
GDH	260	0.027	9630	n.a.	6.5	*Bacillus megaterium*	1	glucose	+++	–	+	[30]
FDH	1.07	3.5	0.31	n.a.	7.0	*Bacillus* sp. F1	1	sodium formate	+	++	+++	[31]
PTDH	0.57	0.74	0.77	n.a.	7.25	*Pseudomonas stutzeri*	1	sodium phosphite	+	++	++	[32]
FNR-QD	0.40[c]	n.a.	n.a.	1.48	7.0	*Chlamydomonas reinhardtii*	3	sodium ascorbate	+	–	+	[33]
Graphene photocat-Rh	0.004[d]	n.a.	n.a.	n.a.	7.0	n.a.	2	triethanol-amine	–	–	–	[34]

[a] TOF = ([substrate]/[catalyst])/time, based on 10 min time points (0.57 μM PSI, 3 mM $NADP^+$). [b] TON = [product]/[catalyst], based on 1 h time points. [c] TOF based on 2 h. [d] TOF based on 348 d^{-1}. [e] Ranking order: +++: Very good, ++: good, +: moderate, –: poor. n.a.: not available. Comparison adapted from reference[5] and this study.

acid and dehydroascorbic acid, respectively, making these reactions atom inefficient. In addition, separation of the compounds from the reaction mixture is laborious and requires additional steps. Thus, the development of an electrode-based electron supply for PSI-Fd-FNR would also allow water oxidation to be coupled to the system as the ultimate electron source (e.g. by PSII[17d]) making it more sustainable and atom efficient.

The biocatalytic potential of the PSI-Fd-FNR cofactor recycling system was evaluated by coupling it to three different oxidoreductases catalyzing the asymmetric reduction of C=C and C=O bonds. As a first proof-of-concept, *Nt*DBR was used for the chemoselective reduction of the C=C bond in *trans*-cinnamaldehyde **1a**, producing dihydrocinnamaldehyde **1b** (Figures 3 and S5).

We chose this double bond reductase over a flavin-dependent ene reductase (ER) to avoid cross reactivity with a flavin cofactor. *Nt*DBR is active with various α,β-unsaturated activated alkenes, and its optimal pH range was determined to be pH 6.4–7.4.[14] *Nt*DBR-catalyzed reactions coupled to PSI-Fd-FNR were carried out at pH 7.0 and 8.0. We only observed reduction product at pH 7.0, confirming the higher activity of *Nt*DBR at this pH value. After 4 h, the conversion of *trans*-cinnamaldehyde was 29.2% (1.49 mM), reaching full conversion within 24 h. Therefore, coupling *Nt*DBR with PSI-Fd-FNR resulted in the steady-state consumption of NADPH, likely limiting the NADPH oxidase activity of FNR previously observed (Figure 2c).

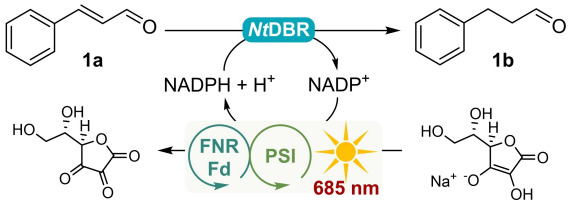

Figure 3. *Nt*DBR-catalyzed reduction of *trans*-cinnamaldehyde **1a** to dihydrocinnamaldehyde **1b** coupled to light-driven PSI-Fd-FNR NADPH recycling.

For the asymmetric reduction of a cyclic ketone, the actinorhodin ketoreductase *act*KR was chosen and coupled to PSI-Fd-FNR (Figure 4a). *act*KR selectively reduces *trans*-1-decalone **2a** to (*S*)-1-decalol **2b**,[15,37] however the substrate used in this reaction was a commercially available 65:35 mixture of *trans*- and *cis*-isomers of 1-decalone, giving the theoretically two (*S*)-products with a maximum conversion of 65% (Figure 4b). Running the reaction with PSI-Fd-FNR over 4 h, we observed two product peaks for 1-decalol **2b** (Figure S6), with 49% conversion. The maximum 65% conversion was reached over 24 h, leaving the *cis*-1-decalone unreacted due to the selectivity of *act*KR.

The PSI-Fd-FNR cofactor recycling system was also coupled with *Lb*ADH for the asymmetric reduction of acetophenone **3a** (Figures 5, S4 and S7), obtaining 3.7 mM of (*R*)-1-phenylethanol **3b** in 4 h. A 24 h reaction afforded full conversion with a product yield of 4.0 mM (*R*)-1-phenylethanol **3b** and no acetophenone left due to evaporation under the current

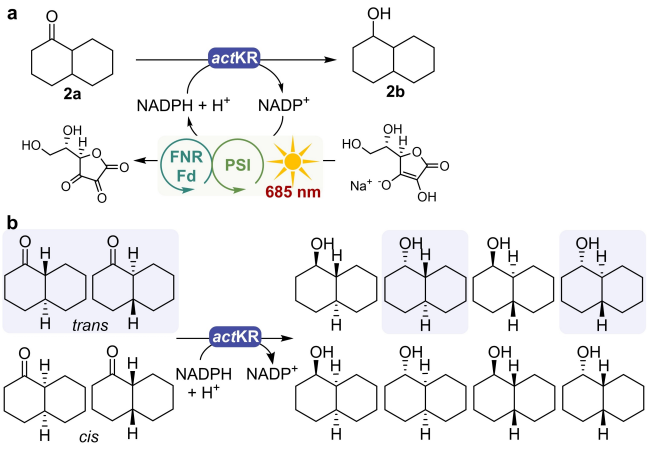

Figure 4. a) *act*KR-catalyzed reduction of 1-decalone **2a** to 1-decalol **2b** coupled to light-driven PSI-Fd-FNR NADPH recycling. b) Expected enantiomers highlighted in violet of (*S*)-1-decalol after *act*KR-catalyzed reduction of *trans*-1-decalone.

Table 2. Biocatalytic conversions of oxidoreductases coupled with the PSI-Fd-FNR cofactor recycling system.[a]

Parameters	Biocatalytic reaction results		
Oxidoreductase	*Nt*DBR	*act*KR	*Lb*ADH
Substrate (5 mM)	*trans*-cinnamaldehyde **1 a**	*trans*-1-decalone **2 a**	acetophenone **3 a**
Product	dihydrocinnamaldehyde 1b	decalol **2 b**	(*R*)-1-phenylethanol **3 b**
4 h PSI-Fd-FNR recycling			
Substrate conversion (%)	29.2 ± 4.6	49.5 ± 0.3	99.3 ± 9.0[b]
Product yield (mM)	1.49 ± 0.24	2.47 ± 0.01	3.73 ± 0.08
24 h PSI-Fd-FNR recycling			
Substrate conversion (%)	> 99.9 ± 8.4	65.3 ± 0.9	93.7 ± 12.8[b]
Product yield (mM)	4.97 ± 0.42	3.26 ± 0.04	3.98 ± 0.02
24 h no PSI (control)			
Substrate conversion (%) no product observed	< 0.1	< 0.1	< 0.1 (3.44 ± 0.02 mM acetophenone left)[b]

[a] Experiments performed in triplicate. [b] High substrate conversion yet incomplete yield observed due to evaporation of acetophenone over 24 h.

reaction set-up. Evaporation was confirmed in a control reaction without PSI, in which the acetophenone concentration displayed a loss of approximately 1 mM over 24 h of incubation under the reaction conditions (Table 2). Improvements to the reaction system would most likely address this issue and allow for a scale-up.

Conclusions

In conclusion, we successfully reconstituted the photosynthetic electron transport chain in vitro for the regeneration of NADPH. $NADP^+$ reduction by PSI-Fd-FNR was best at pH 7.5, reaching a turnover frequency of 2.55 s^{-1} (> 9000 h^{-1}). We observed no difference in the NADPH production rate under aerobic and anaerobic conditions. Instead, a faster decline of NADPH over time under aerobic conditions was ascribed to FNR oxidation activity and cofactor decomposition when unused. To prove applicability, PSI-Fd-FNR was coupled to *Nt*DBR, *act*KR, and *Lb*ADH, achieving full conversion without affecting enantioselectivity. The light-driven NADPH generation afforded a TON of 3050, thus, we demonstrated the capacity of PSI-Fd-FNR to drive continuous NADPH-dependent biocatalytic conversions.

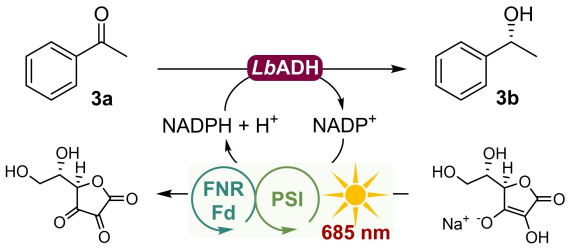

Figure 5. *Lb*ADH-catalyzed reduction of acetophenone **3 a** to (*R*)-1-phenylethanol **3 b** coupled to light-driven PSI-Fd-FNR NADPH recycling.

Experimental Section

Enzymes purification

Enzymes were produced and purified as previously reported: PSI from *Thermosynechococcus vestitus* BP1 (formerly known as *T. longatus* BP-1),[38] double bond reductase from *Nicotiana tabacum* (*Nt*DBR),[14] actinorhodin ketoreductase from *Streptomyces coelicolor* (*act*KR),[37] alcohol dehydrogenase from *Lactobacillus brevis* (*Lb*ADH).[39] The genes of Fd and FNR from *T. vestitus* BP1 were recombinantly expressed in BL21 Δ*iscR* and BL21, respectively, and subsequently purified by affinity chromatography.[40]

Determination of NADPH production rate of PSI-Fd-FNR biocascade

Reaction conditions: 100 mM sodium ascorbate (NaAsc), 0.8 mM dichlorophenolindophenol (DCPIP), 50 μg chlorophyll (Chl) equivalent photosystem I (PSI), 4 μM ferredoxin (Fd), 1 μM of ferredoxin $NADP^+$ reductase (FNR), 3 mM $NADP^+$. Different pH and buffer conditions were used based on the type of biocatalytic reaction: 50 mM MOPS-NaOH pH 7.0, 50 mM Tris-HCl pH 7.5 or 50 mM Tricine buffer pH 8.0 with 30 mM NaCl and 0.03 % *n*-dodecyl-β-maltoside in a reaction volume of 1 mL. Unless otherwise mentioned, all reactions were performed under anaerobic conditions at room temperature (25 °C to 31 °C), shaken at 100 rpm. $NADP^+$ reduction was initiated by illumination with red light (λ = 685 nm, 500 μmol m^{-2} s^{-1}). For estimation of the produced NADPH, an aliquot of 30 μL of the reaction medium was collected after 0, 10, 30 min, 1, 2, 4, and 6 h of incubation. The collected reaction medium was centrifuged with a 3 kDa Centricon™ filter to remove all protein components. The concentration step was performed until the volume was reduced to < 20 μL. The flow-through was stored at −20 °C until future use.

The amount of NADPH was quantified by fluorescence spectroscopy (Edinburgh Instruments FLS900) using a quartz cuvette with 1 cm path length. 2 μL of the above flow through was diluted to 2 mL, and then the measurement was performed. The sample was excited at 340 nm and emission spectra were recorded from 350 to 650 nm. The set parameters were dwell time 0.10 s, lamp Xe900, temperature 25 °C, scan slit: 1.9980, detector R928. The standard curve was established by serial dilution of NADPH (0 to 6 μM). The standard curve with corresponding NADPH concentrations and fluorescence range are as shown (Figure S3). Based on the standard curve, the NADPH production rate of the PSI-Fd-FNR biocascade was estimated. Each subjected sample value represents the average of 5 scan repeats of 3 individual replicates.

Determination of activity of the PSI-Fd-FNR biocascade

The $NADP^+$ reduction activity of the PSI-Fd-FNR biocascade was determined based on the NADPH concentration at 10 min time point of the reaction. The determined activity of PSI-Fd-FNR system was 0.092 U and 0.087 U at pH 7 and pH 7.5, respectively. The TOF and TON values were obtained by normalization of enzyme units of the PSI-Fd-FNR biocascade with respect to the time point and concentration of PSI.

Coupling of PSI-Fd-FNR NADPH recycling system

Biotransformation reactions of *Nt*DBR, *act*KR, and *Lb*ADH were carried out with the PSI-Fd-FNR NADPH recycling system. Reaction conditions: 100 mM NaAsc, 0.8 mM DCPIP, 50 mg Chl equivalent PSI, 4 μM Fd, 1 μM FNR, 3 mM $NADP^+$, 30 mM NaCl, 0.03% β-DM, 5 μM enzyme (Table 3), 5 mM substrate, buffer (Table 3), reaction volume: 1 mL, incubation time: 24 h, room temperature (25 °C to 31 °C), 100 rpm, inert atmosphere. Depending on the enzyme, the corresponding substrate and buffer were used (Table 3).

To quench the biocatalytic reactions, the reaction medium was filtered through a 3 kDa cut-off filter until the protein volume reached <50 μL. The flow-through sample was extracted with 500 μL ethyl acetate containing 5 mM dodecane (internal standard), and was vortexed and centrifuged (13,000 rpm, 10 °C, 4 min). The organic phase was separated, dried over anhydrous $MgSO_4$, transferred to a GC vial and analyzed by GC-FID with calibration curves. Bioconversion was assessed at 4 and 24 h of reaction time (Table 2).

Supporting Information

Additional information on electron transfer and protein-protein interactions in PSI-Fd-FNR biocascade, biotransformations, GC analyses, supplementary figures, including references.[41,42]

Acknowledgements

This project received funding from the European Union's Horizon 2020 research and innovation programme under the Marie Skłodowska-Curie grant agreement No 764920, as well as the Deutsche Forschungsgemeinschaft (DFG)-funded Research Training Group 2341 "Microbial Substrate Conversion (MiCon)". The authors are grateful to E. P. J. Jongkind and A. E. Wolder for providing purified enzymes *Lb*ADH and *Nt*DBR. Open Access funding enabled and organized by Projekt DEAL.

Conflict of Interests

The authors declare no conflict of interest.

Table 3. Substrate concentration and buffers.

Enzyme (5 μM)	[Substrate] (5 mM)	Buffer
*act*KR	*cis/trans*-1-decalone	50 mM Tris-HCl pH 7.5
*Nt*DBR	*trans*-cinnamaldehyde	50 mM MOPS-NaOH pH 7.0
*Lb*ADH	acetophenone	50 mM Tris-HCl pH 7.5

Data Availability Statement

The data that support the findings of this study are available from the corresponding author upon reasonable request.

Keywords: biocascades · enzymatic reduction · ferredoxin $NADP^+$ oxidoreductase · NADPH cofactor regeneration · photobiocatalysis

[1] a) S. K. Wu, R. Snajdrova, J. C. Moore, K. Baldenius, U. T. Bornscheuer, *Angew. Chem. Int. Ed.* **2021**, *60*, 88–119; b) C. K. Winkler, J. H. Schrittwieser, W. Kroutil, *ACS Cent. Sci.* **2021**, *7*, 55–71; c) U. Hanefeld, F. Hollmann, C. E. Paul, *Chem. Soc. Rev.* **2022**, *51*, 594–627.
[2] L. Sellés Vidal, C. L. Kelly, P. M. Mordaka, J. T. Heap, *Biochim. Biophys. Acta Proteins Proteomics* **2018**, *1866*, 327–347.
[3] a) H. K. Chenault, G. M. Whitesides, *Appl. Biochem. Biotechnol.* **1987**, *14*, 147–197; b) A. Guarneri, W. J. H. van Berkel, C. E. Paul, *Curr. Opin. Biotechnol.* **2019**, *60*, 63–71.
[4] S. Mordhorst, J. N. Andexer, *Nat. Prod. Rep.* **2020**, *37*, 1316–1333.
[5] L. Lauterbach, O. Lenz, K. A. Vincent, *FEBS J.* **2013**, *280*, 3058–3068.
[6] a) K. Köninger, Á. Gómez Baraibar, C. Mügge, C. E. Paul, F. Hollmann, M. M. Nowaczyk, R. Kourist, *Angew. Chem. Int. Ed.* **2016**, *55*, 5582–5585; b) L. Assil-Companioni, H. C. Buchsenschutz, D. Solymosi, N. G. Dyczmons-Nowaczyk, K. K. F. Bauer, S. Wallner, P. Macheroux, Y. Allahverdiyeva, M. M. Nowaczyk, R. Kourist, *ACS Catal.* **2020**, *10*, 11864–11877; c) E. Erdem, L. Malihan-Yap, L. Assil-Companioni, H. Grimm, G. D. Barone, C. Serveau-Avesque, A. Amouric, K. Duquesne, V. de Berardinis, Y. Allahverdiyeva, V. Alphand, R. Kourist, *ACS Catal.* **2022**, *12*, 66–72.
[7] M. Hobisch, J. Spasic, L. Malihan-Yap, G. D. Barone, K. Castiglione, P. Tamagnini, S. Kara, R. Kourist, *ChemSusChem* **2021**, *14*, 3219–3225.
[8] a) P. Jordan, P. Fromme, H. T. Witt, O. Klukas, W. Saenger, N. Krauss, *Nature* **2001**, *411*, 909–917; b) A. Badura, D. Guschin, T. Kothe, M. J. Kopczak, W. Schuhmann, M. Rogner, *Energy Environ. Sci.* **2011**, *4*, 2435–2440.
[9] R. Mutoh, N. Muraki, K. Shinmura, H. Kubota-Kawai, Y. H. Lee, M. M. Nowaczyk, M. Rogner, T. Hase, T. Ikegami, G. Kurisu, *Biochemistry* **2015**, *54*, 6052–6061.
[10] P. Liauw, T. Mashiba, M. Kopczak, K. Wiegand, N. Muraki, H. Kubota, Y. Kawano, M. Ikeuchi, T. Hase, M. Rogner, G. Kurisu, *Acta Crystallogr. Sect. F* **2012**, *68*, 1048–1051.
[11] M. Ihara, Y. Kawano, M. Urano, A. Okabe, *PLoS One* **2013**, *8*, e71581.
[12] N. Cassan, B. Lagoutte, P. Setif, *J. Biol. Chem.* **2005**, *280*, 25960–25972.
[13] C. E. Lubner, A. M. Applegate, P. Knorzer, A. Ganago, D. A. Bryant, T. Happe, J. H. Golbeck, *Proc. Nat. Acad. Sci.* **2011**, *108*, 20988–20991.
[14] D. J. Mansell, H. S. Toogood, J. Waller, J. M. X. Hughes, C. W. Levy, J. M. Gardiner, N. S. Scrutton, *ACS Catal.* **2013**, *3*, 370–379.
[15] P. Javidpour, J. Bruegger, S. Srithahan, T. P. Korman, M. P. Crump, J. Crosby, M. D. Burkart, S. C. Tsai, *Chem. Biol.* **2013**, *20*, 1225–1234.
[16] S. Leuchs, L. Greiner, *Chem. Biochem. Eng. Q.* **2011**, *25*, 267–281.
[17] a) A. Petrova, M. Mamedov, B. Ivanov, A. Semenov, M. Kozuleva, *Photosynth. Res.* **2018**, *137*, 421–429; b) D. Dvoranová, Z. Barbieriková, S. Dorotikova, M. Malcek, A. Brincko, L. Rispanová, L. Bucinsky, A. Stako, V. Brezová, P. Rapta, *J. Solid State Electrochem.* **2015**, *19*, 2633–2642; c) J. S. Fruton, *J. Biol. Chem.* **1934**, *105*, 79–85; d) T. Kothe, N. Plumeré, A. Badura, M. M. Nowaczyk, D. A. Guschin, M. Rogner, W. Schuhmann, *Angew. Chem. Int. Ed.* **2013**, *52*, 14233–14236; e) A. Badura, T. Kothe, W. Schuhmann, M. Rogner, *Energy Environ. Sci.* **2011**, *4*, 3263–3274.
[18] a) D. M. Kramer, C. A. Sacksteder, J. A. Cruz, *Photosynth. Res.* **1999**, *60*, 151–163; b) M. D. L. Trinh, S. Masuda, *Front. Plant Sci.* **2022**, *13*, 919896.
[19] a) P. Q. Y. Setif, H. Bottin, *Biochemistry* **1994**, *33*, 8495–8504; b) J. Li, N. Hamaoka, F. Makino, A. Kawamoto, Y. Lin, M. Rogner, M. M. Nowaczyk, Y. H. Lee, K. Namba, C. Gerle, G. Kurisu, *Commun. Biol.* **2022**, *5*, 951.
[20] a) P. Fromme, A. Melkozernov, P. Jordan, N. Krauss, *FEBS Lett.* **2003**, *555*, 40–44; b) T. Takabe, H. Ishikawa, S. Niwa, S. Itoh, *J. Biochem.* **1983**, *94*, 1901–1911.
[21] G. Wittenberg, W. Sheffler, D. Darchi, D. Baker, D. Noy, *Phys. Chem. Chem. Phys.* **2013**, *15*, 19608–19614.
[22] N. Carrillo, E. A. Ceccarelli, *Eur. J. Biochem.* **2003**, *270*, 1900–1915.
[23] K. Jensen, J. B. Johnston, P. R. O. de Montellano, B. L. Moller, *Biotechnol. Lett.* **2012**, *34*, 239–245.

[24] K. Nguyen, B. D. Bruce, *Biochim. Biophys. Acta Bioenerg.* **2014**, *1837*, 1553–1566.
[25] a) G. E. Milanovsky, A. A. Petrova, D. A. Cherepanov, A. Y. Semenov, *Photosynth. Res.* **2017**, *133*, 185–199; b) P. Sétif, *Biochim. Biophys. Acta Bioenerg.* **2001**, *1507*, 161–179.
[26] M. Faro, S. Frago, T. Mayoral, J. A. Hermoso, J. Sanz-Aparicio, C. Gomez-Moreno, M. Medina, *Eur. J. Biochem.* **2002**, *269*, 4938–4947.
[27] R. Masaki, K. Wada, H. Matsubara, *J. Biochem.* **1979**, *86*, 951–962.
[28] M. I. Karayannis, *Talanta* **1976**, *23*, 27–30.
[29] J. T. Wu, L. H. Wu, J. A. Knight, *Clin. Chem.* **1986**, *32*, 314–319.
[30] T. Nagao, Y. Makino, K. Yamamoto, I. Urabe, H. Okada, *FEBS Lett.* **1989**, *253*, 113–116.
[31] H. T. Ding, D. F. Liu, Z. L. Li, Y. Q. Du, X. H. Xu, Y. H. Zhao, *J. Appl. Microbiol.* **2011**, *111*, 1075–1085.
[32] L. Zhang, E. King, W. B. Black, C. M. Heckmann, A. Wolder, Y. Cui, F. Nicklen, J. B. Siegel, R. Luo, C. E. Paul, H. Li, *Nat. Commun.* **2022**, *13*, 5021.
[33] K. A. Brown, M. B. Wilker, M. Boehm, H. Hamby, G. Dukovic, P. W. King, *ACS Catal.* **2016**, *6*, 2201–2204.
[34] S. Choudhury, J.-O. Baeg, N.-J. Park, R. K. Yadav, *Green Chem.* **2014**, *16*, 4389–4400.
[35] T. Fujii, E. Yokoyama, K. Inoue, H. Sakurai, *Biochim. Biophys. Acta* **1990**, *1015*, 41–48.
[36] P. Wang, A. Frank, F. Zhao, J. Szczesny, J. R. C. Junqueira, S. Zacarias, A. Ruff, M. M. Nowaczyk, I. A. C. Pereira, M. Rogner, F. Conzuelo, W. Schuhmann, *Angew. Chem. Int. Ed.* **2021**, *60*, 2000–2006.
[37] S. A. Serapian, M. W. van de Kamp, *ACS Catal.* **2019**, *9*, 2381–2394.
[38] E. El-Mohsnawy, M. J. Kopczak, E. Schlodder, M. M. Nowaczyk, H. E. Meyer, B. Warscheid, N. v. Karapetyan, M. Rögner, *Biochemistry* **2010**, *49*, 4740–4751.
[39] N. Adebar, H. Gröger, *BioEngineering* **2019**, *6*, 1–26.
[40] H. Medipally, M. Mann, C. Kötting, W. J. H. van Berkel, M. M. Nowaczyk, *ChemBioChem* **2023**, *24*, e202300025.
[41] I. Caspy, A. Borovikova-Sheinker, D. Klaiman, Y. Shkolnisky, N. Nelson, *Nat. Plants* **2020**, *6*, 1300–1305.
[42] G. Kurisu, M. Kusunoki, E. Katoh, T. Yamazaki, K. Teshima, Y. Onda, Y. Kimata-Ariga, T. Hase, *Nat. Struct. Biol.* **2001**, *8*, 117–121.

Manuscript received: July 1, 2023
Revised manuscript received: July 5, 2023
Accepted manuscript online: July 6, 2023
Version of record online: ■■, ■■

RESEARCH ARTICLE

Lights on! Illuminated photosystem I, coupled to ferredoxin and ferredoxin reductase, drives continuous NADPH-dependent biocatalytic conversions for asymmetric reductions.

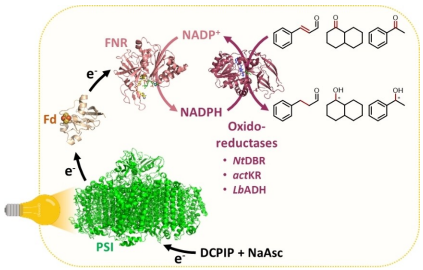

H. Medipally, Dr. A. Guarneri, L. Pospisil, Prof. Dr. M. C. R. Franssen, Prof. Dr. W. J. H. van Berkel, Prof. Dr. C. E. Paul, Prof. Dr. M. M. Nowaczyk**